See related commentary on pg 1854

Hemidesmosomes and Focal Adhesions Treadmill as Separate but Linked Entities during Keratinocyte Migration

Anne Pora[1], Sungjun Yoon[1], Reinhard Windoffer[1] and Rudolf E. Leube[1]

Hemidesmosomes anchor the epidermal keratin filament cytoskeleton to the extracellular matrix. They are crucial for the mechanical integrity of skin. Their role in keratinocyte migration, however, remains unclear. Examining migrating primary human keratinocytes, we find that hemidesmosomes cluster as ordered arrays consisting of multiple chevrons that are flanked by actin-associated focal adhesions. These hemidesmosomal arrays with intercalated focal adhesions extend from the cell rear to the cell front. New hemidesmosomal chevrons form subsequent to focal adhesion assembly at the cell's leading front, whereas chevrons and associated focal adhesions disassemble at the cell rear in reverse order. The bulk of the hemidesmosome-focal adhesion composite, however, remains attached to the substratum during cell translocation. Similar hemidesmosome-focal adhesion patterns emerge on X-shaped fibronectin-coated micropatterns, during cell spreading and in leader cells during collective cell migration. We further find that hemidesmosomes and focal adhesions affect each other's distribution. We propose that both junctions are separate but linked entities, which treadmill coordinately to support efficient directed cell migration and cooperate to coordinate the dynamic interplay between the keratin and actin cytoskeleton.

Journal of Investigative Dermatology (2019) **139,** 1876–1888; doi:10.1016/j.jid.2019.03.1139

INTRODUCTION

Epithelial cell migration is a key process in physiological situations, such as tissue morphogenesis, and in pathological situations, such as wound healing or cancer metastasis. The linkage of the cytoskeleton to extracellular matrix (ECM) contacts provides the leverage for cellular translocation over a substrate. Repeated cycles of protrusion at the front and contraction at the back are accompanied by cycles of assembly and disassembly of cell-ECM contacts (Lauffenburger and Horwitz, 1996). ECM contact sites are grouped into focal adhesions (FAs) and hemidesmosomes (HDs). FAs consist of different integrin heterodimers, actin binding proteins, and many associated linker and signaling proteins (Zaidel-Bar and Geiger, 2010; Zaidel-Bar et al., 2007). They serve as bidirectional hubs for multiple signaling pathways integrating signals from the inside and outside of cells. By sensing mechanical characteristics of the environment FAs play crucial roles in regulating cell migration (Geiger and Yamada, 2011).

Much less attention has been paid to HDs, epithelial-specific cell–ECM adhesions that are linked to the keratin intermediate filament cytoskeleton (Chaudhari and Vaidya, 2015; Hopkinson et al., 2014; Walko et al., 2015). They are characterized by HD-specific α6/β4 integrin heterodimers, which are connected through plakins to keratins (Nahidiazar et al., 2015). HDs are considered to be responsible for the mechanical integrity of epithelial tissues, because mutations of HD proteins lead to skin blistering diseases (Tsuruta et al., 2011).

It was initially thought that FAs have a pro-migratory role as highly dynamic structures, whereas HDs inhibit migration as highly stable ECM attachment sites (e.g., Carter et al., 1990; Rabinovitz et al., 1999). This simple view, however, has been challenged by live cell imaging revealing highly dynamic HDs in migrating cells (Geuijen and Sonnenberg, 2002; Hiroyasu et al., 2016; Osmani et al., 2018; Ozawa et al., 2010; Tsuruta et al., 2003). These analyses further suggested that, instead, the intricate crosstalk between FAs and HDs regulates speed and persistence of cell migration.

The current study focuses on the crosstalk between HDs and FAs examining primary human epidermal keratinocytes during cell migration. We show that HDs and FAs are organized in a hitherto unknown, highly ordered pattern consisting of aligned hemidesmosomal chevrons with intercalated FAs that are oriented in the direction of migration. The overall arrangement is characterized by topologically defined regions of assembly at the cell front, stability in the cell center and disassembly in the rear to support directed translocation of the cell body. The close-knit relationship between HDs and FAs is also observed on micropatterns, during cell spreading and in leader cells during collective cell migration. In accordance, interference with either HDs or FAs results in perturbation of the other. Taken together, our study maps out the spatially and temporally coordinated crosstalk between FAs and HDs as a major facilitator of efficient keratinocyte migration.

[1]*Institute of Molecular and Cellular Anatomy, Rheinisch-Westfälische Technische Hochschule Aachen University, Aachen, Germany*

Correspondence: Rudolf E. Leube, Institute of Molecular and Cellular Anatomy, Rheinisch-Westfälische Technische Hochschule Aachen University, Wendlingweg 2, 52074 Aachen, Germany. E-mail: rleube@ukaachen.de

Abbreviations: ECM, extracellular matrix; FA, focal adhesion; HD, hemidesmosome; nHEK, normal human epidermal keratinocyte

Received 4 October 2018; revised 18 March 2019; accepted 19 March 2019; accepted manuscript published online 2 April 2019; corrected proof published online 29 July 2019

RESULTS

Hemidesmosomal proteins cluster in chevron-shaped arrays in migrating primary human keratinocytes

Primary normal human epidermal keratinocytes (nHEKs) migrate spontaneously when seeded on fibronectin-coated glass coverslips at low density. They adopt a D-shape with a large lamellipodium at the front and a straight rear-end. Immunostaining against HD-specific β4 integrin uncovered a highly ordered pattern consisting of chevron-shaped arrays (Figure 1a). The arrays extend from the cell rear towards the semi-circular lamellipodial leading edge. The same pattern was observed with antibodies against α6 integrin, which associates with β4 integrin in HDs (Figure 1b). To show that the α6/β4 integrin–positive sites are HD-like structures, co-immunostaining was performed for β4 integrin with hemidesmosomal plakin-type plaque proteins BP230 and plectin. Extensive co-localization was detected for BP230 (Figure 1c). The anti-plectin staining also showed extensive co-localization, but extended beyond because of the additional non-hemidesmosomal distribution of plectin (Wiche et al., 2015). Double immunofluorescence microscopy further showed that the β4 integrin–positive chevrons were in close apposition to keratin intermediate filaments (Figure 1e, Supplementary Figure S1 online). Taken together, we conclude that chevrons are a unique type of hemidesmosomal arrangement that is specific for migrating keratinocytes.

Hemidesmosomal chevron arrays and focal adhesion sites are spatially linked but segregated

To examine the relationship between hemidesmosomal chevrons and actin-anchoring FAs in migrating nHEKs, fluorescence microscopy analyses were performed (Figure 2a). They revealed that paxillin-positive and actin stress fiber-associated FAs are intercalated between hemidesmosomal chevrons. Actin fibers were clearly excluded from β4 integrin-positive patches. Together, HDs and FAs formed regularly patterned superstructures. To more precisely examine their spatial relationship, nHEKs were seeded on X-shaped micropatterned fibronectin islands. Immunostaining showed that β4 integrin clustered in chevron-like structures, which were arranged symmetrically along the four arms of the pattern (Figure 2b). Chevrons increased in size towards the cell center. Anti-paxillin staining further revealed that FAs were precisely localized between the hemidesmosomal chevrons. As expected, FAs were associated with prominent actin stress fibers, while hemidesmosomal chevrons were not. When nHEKs were grown on fibronectin-coated D-shaped patterns, a different yet still non-overlapping distribution of hemidesmosomal and FA proteins was detected (Supplementary Figure S2 online). β4 integrin signal was detected in a broad circumferential region with multiple indentations on both sides harboring FAs. The outer FA-rich region consisted of small attachment sites and was directly next to the actin-rich cell cortex, while larger, actin stress fiber-associated FAs localized to the gaps along the inner border of the HD region.

Focal adhesion-decorated hemidesmosomal chevrons are formed at the cell front and are removed in the cell rear in migrating keratinocytes

Time-lapse fluorescence microscopy was done to study HD and FA dynamics in migrating nHEKs. To this end, nHEKs were co-transfected with a β4 integrin-eGFP and a paxillin-DsRed construct to label HDs and FAs, respectively. Assembly of FAs and HDs was exclusively detected at the cell front (Figure 3a). Paxillin-positive nascent FAs appeared first (Figure 3b, Supplementary Movies S1, S2 online). They subsequently enlarged into ellipsoid FAs at the lamellipodium-lamellum interface. Pairs of ellipsoid FAs typically faced each other. They were arranged at an oblique angle to the direction of migration. The space between FAs was subsequently filled with hemidesmosomal β4 integrin extending the pre-existing chevron-like structures towards the cell front with FA enlargement occurring concurrently. Once the characteristic FA-HD chevron pattern was established, it stayed in place with respect to the substratum without positional changes of its components (Figure 3c, Supplementary Movie S1). Yet, the size and shape of individual FAs were subject to variation. The continuous growth of the FA-HD chevrons at the cell front was paralleled by translocation of the cell body in the direction of migration. As a result old FA-HD chevrons, which remained tightly attached to the substratum, became localized towards the cell rear. At the very back of the chevron arrays, a slight sliding of FAs occurred, eventually leading to removal of paxillin-positive structures just prior to retraction fiber formation (Supplementary Movie S1, Figure 3c). Typically, β4 integrin–positive regions persisted until retraction fibers were ripped off leaving behind substratum-attached β4 integrin patches (see also Figure 2a). Figure 3d summarizes the observed morphogenesis and removal of the FA-HD chevron pattern.

Hemidesmosomal chevron patterns form during cell spreading and polarization

The formation of hemidesmosomal chevrons in the leading front of migrating cells suggested that a similar process may occur in nHEKs during spreading and subsequent polarization. To test this idea, nHEKs were placed on fibronectin-coated glass slides and fixed after defined time intervals for staining (Figure 4a). Thirty minutes after seeding, cells were circular, presenting multiple paxillin-positive FAs in the cell periphery that were associated with phalloidin-positive actin filaments. At this time point, only a multipunctate and disordered β4 integrin distribution was detectable in the cell center. By 75 minutes, cells had spread and FAs were not any more restricted to the outermost cell periphery. Conversely, β4 integrin–positive structures had formed nearby with no visible overlap, but alignment of both adhesion sites had emerged (arrows at 75 minutes after seeding in Figure 4a and enlargement in Figure 4b). One hundred and sixty-five minutes after seeding, cells started to migrate. By this time, aligned chevrons were discernible in the entire leading cell front (Figure 4b).

To find out how the morphogenesis of HD chevrons relates to keratin network organization, spreading cells were co-stained for β4 integrin and keratin. Co-localization was obvious 45 minutes after seeding when HD-like structures

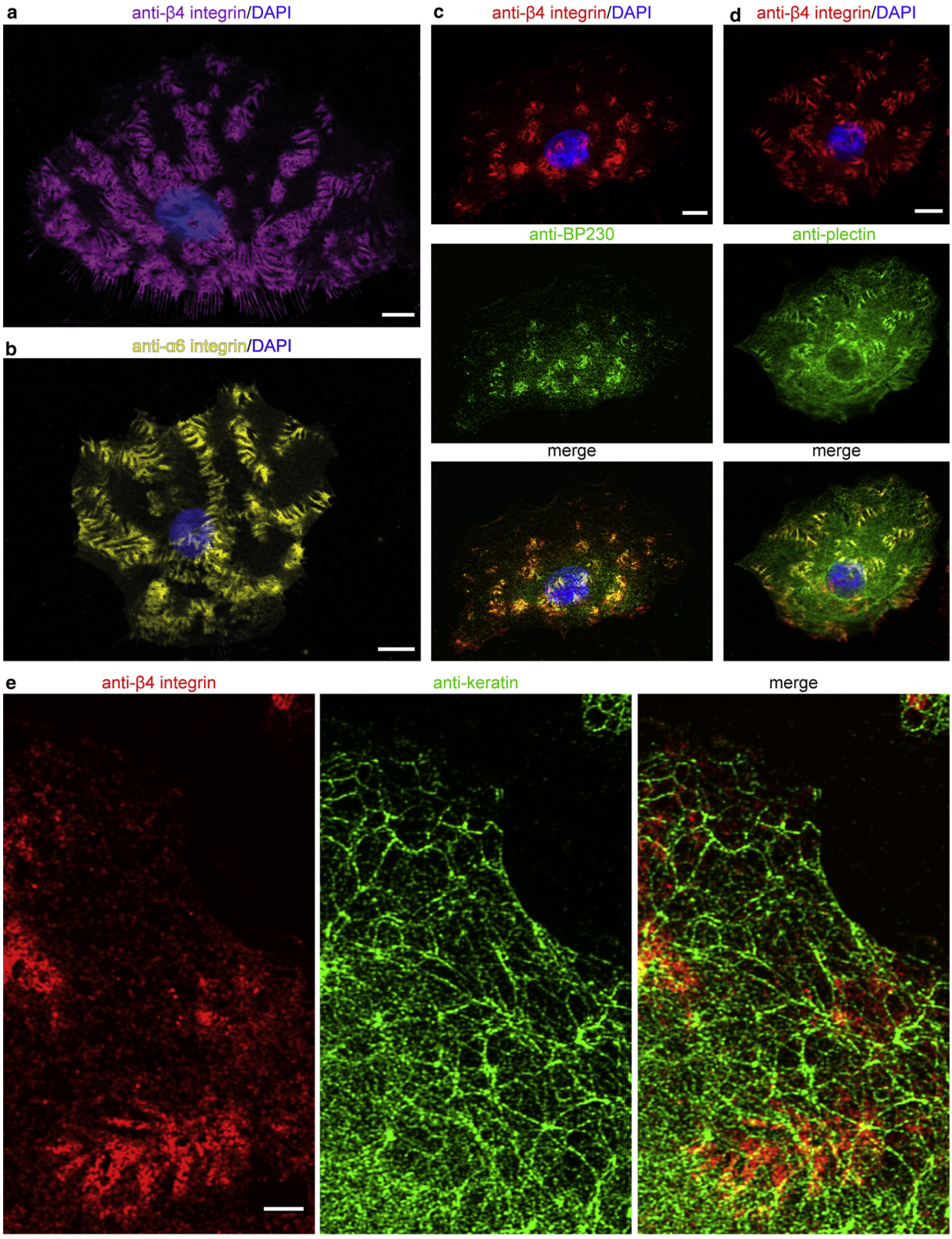

Figure 1. Hemidesmosomal proteins localize to arrays of chevron-shaped structures in migrating normal human epithelial keratinocytes. The immunofluorescence images (**a**–**d**, epifluorescence microscopy, scale bars = 10 μm; **e**, confocal laser scanning microscopy, scale bars = 2.5 μm) depict single polarized normal human epithelial keratinocytes 2 days after seeding on fibronectin-coated glass coverslips. (**a, b**) Anti-β4 and anti-α6 integrin antibodies stain similar arrays consisting of aligned chevron-shaped structures radiating from the rear to the front. (**c, d**) Anti-β4 integrin antibodies co-localize with anti-BP230 (**c**) and anti-plectin antibodies (**d**) in chevron-like structures **(e)** show maximum intensity projections recording anti-β4 integrin and anti-keratin immunofluorescence in the front of a migrating normal human epithelial keratinocytes (further details in Supplementary Figure S1).

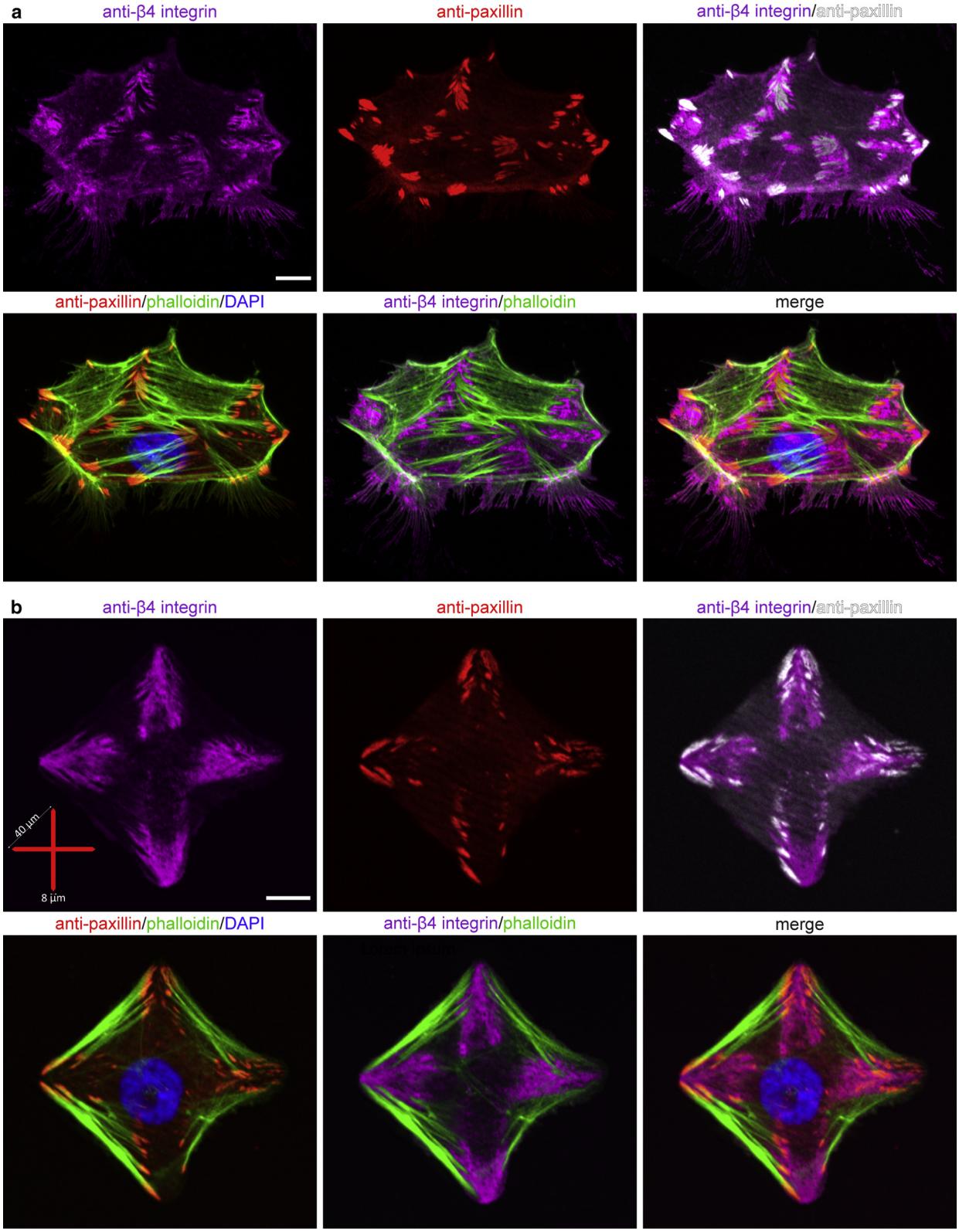

Figure 2. Focal adhesions intercalate in hemidesmosomal chevrons in migrating keratinocytes and keratinocytes grown on X-shaped micropatterns. Quadruple epifluorescence images show anti-β4 integrin immunofluorescence, anti-paxillin immunofluorescence, Alexa 488 phalloidin labeling and DAPI labeling either alone or in different combinations (false white color for anti-paxillin fluorescence) in single normal human epithelial keratinocytes. (**a**) Normal human epithelial keratinocytes were seeded on fibronectin-coated glass coverslips and fixed with paraformaldehyde and acetone after 2 days, prior to labeling. (**b**) Normal human epithelial keratinocytes were seeded on fibronectin-coated X-micropatterns and were fixed after 1 day with paraformaldehyde and acetone before labeling. Note that paxillin-positive focal adhesions align next to but do not overlap with β4 integrin-positive hemidesmosomal chevrons. Furthermore, actin stress fibers associate selectively with paxillin-positive structures. Scale bars = 10 μm.

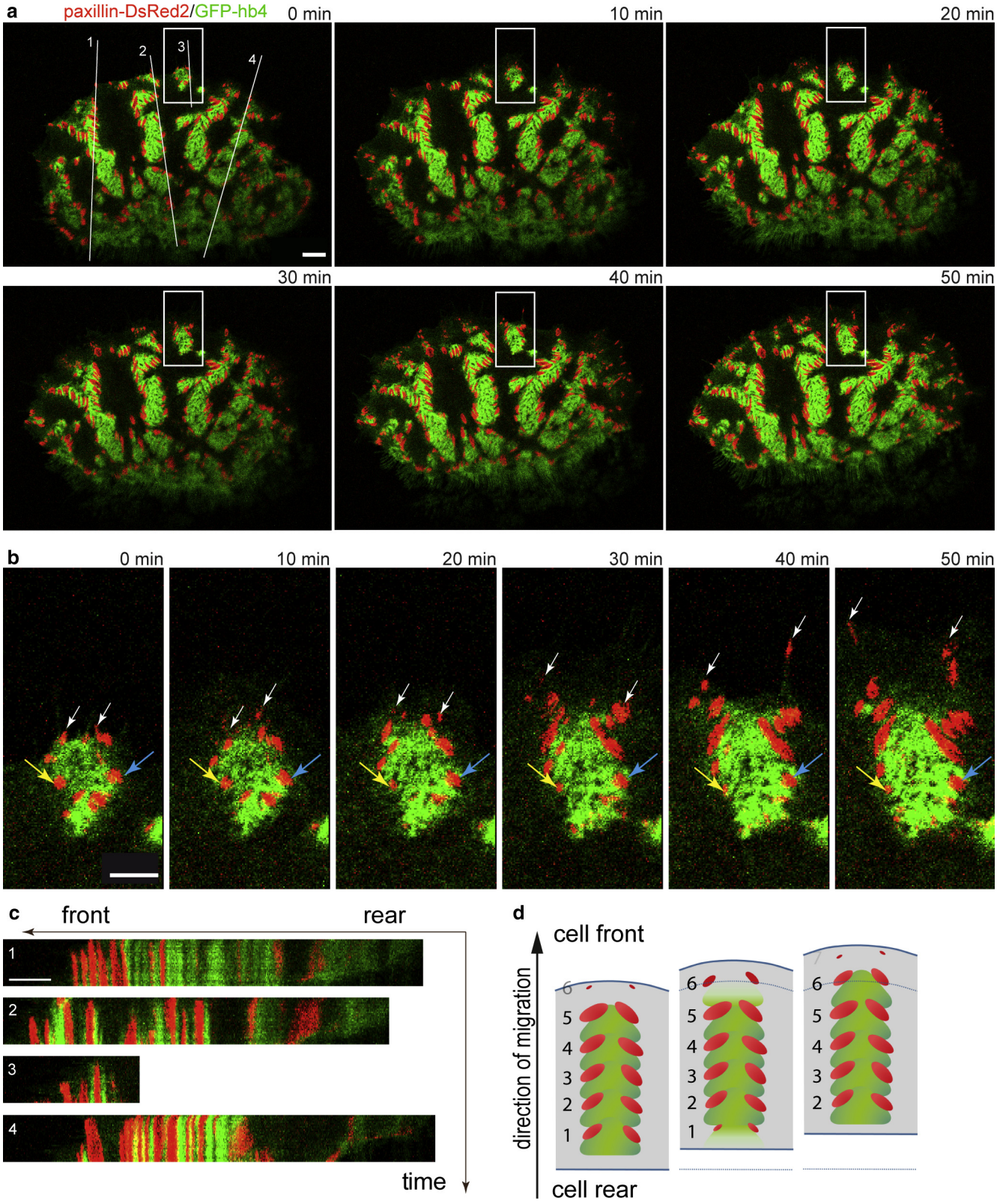

Figure 3. Focal adhesions and hemidesmosomes treadmill coordinately during keratinocyte migration. Time-lapse fluorescence confocal microscopy of a migrating nHEK producing GFP-β4 integrin (GFP-hb4) and paxillin-DsRed2 (complete image series in Supplementary Movies S1, S2). (**a**) Paxillin-positive focal adhesions form near the front prior to the appearance of nearby but non-overlapping β4 integrin–positive patches. (**b**) Magnification of boxed area; nascent focal adhesions marked by white arrows. Note the subsequent positional stability of the hemidesmosomal chevrons with intercalated focal adhesions (yellow and blue arrows) until paxillin-positive focal adhesions are removed prior to β4 integrin in the cell rear. **(c)** The kymograms were prepared along the lines shown in (**a**). Scale bars = 10 μm in (**a**); 5 μm in (**b**); and 3 μm in (**c**). (**d**) Summary scheme of hemidesmosome-focal adhesion dynamics.

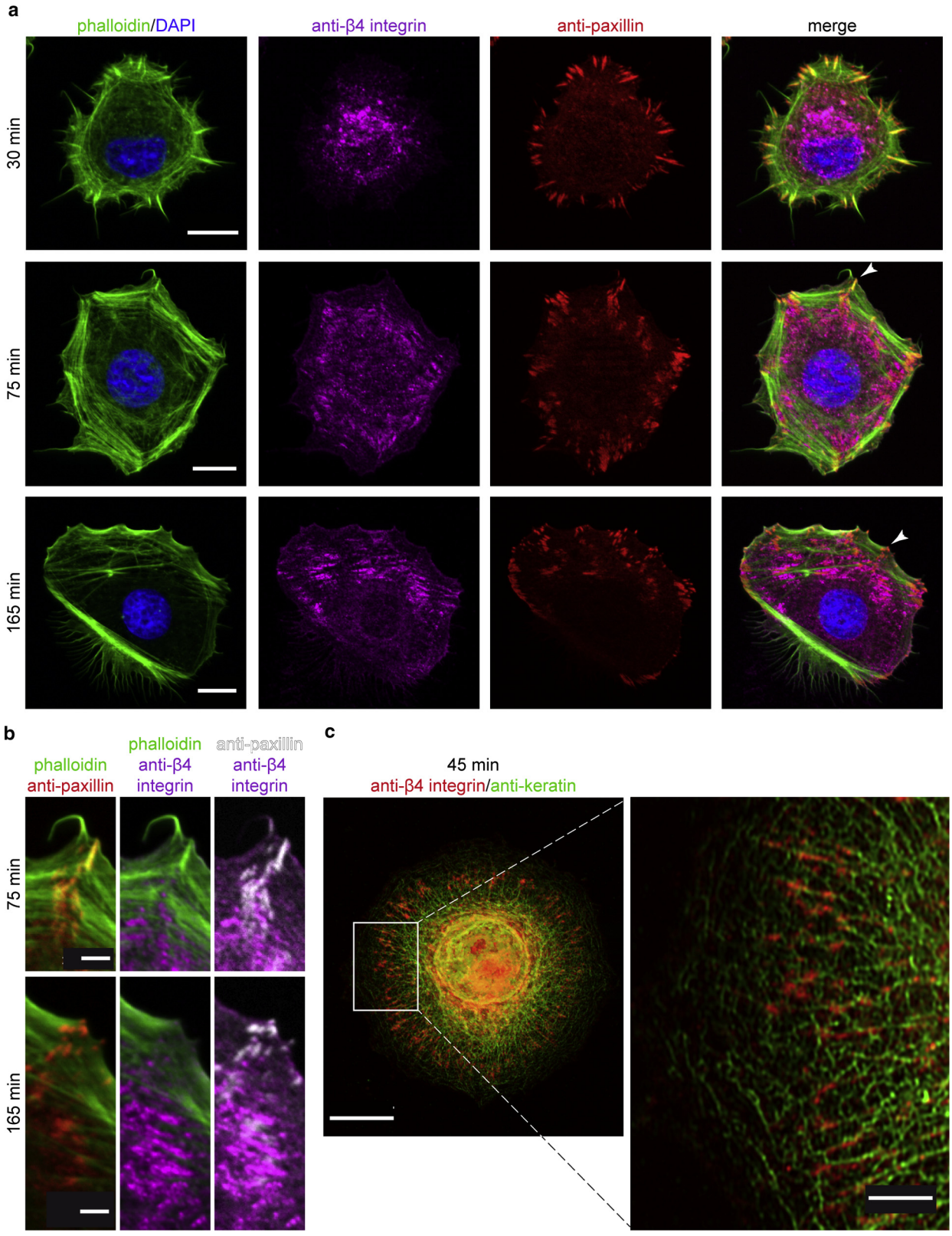

Figure 4. Chevron-like hemidesmosomes are formed next to focal adhesions and in association with keratin filaments during substrate adhesion. (**a**) Quadruple epifluorescence microscopy of single normal human epithelial keratinocytes at different times after seeding. Note that actin fiber-associated paxillin-positive focal adhesions appear in the periphery, moving toward the center during maturation, while β4 integrin is initially localized centrally accumulating later close to focal adhesions during polarization (enlargements in **b**). (**c**) Immunofluorescence of normal human epithelial keratinocytes 45 minutes after seeding (left, maximum intensity projection of entire cell; right, single focal plane of delineated area). Note the abundant perinuclear keratin with radial filaments attached to β4 integrin–positive dots and variably sized keratin particles in the periphery. Scale bars = 10 μm in (**a**, **c**) (left); 2.5 μm in (**b**, **c**) (right).

started to appear. Each of the β4 integrin dots in the cell periphery was associated with radial keratin intermediate filaments (Figure 4c). In the outermost part of the spreading cells, many small filamentous keratin particles, known to correspond to nascent keratin intermediate filaments (Windoffer et al., 2011), were seen in the vicinity of new FAs.

Focal adhesions and hemidesmosomes affect each other's distribution during chevron pattern formation

To test whether HD chevrons were able to form when FA formation was impaired, nHEKs were treated with anti-β1 integrin blocking antibody (Figure 5a). Although fewer cells adhered, FAs still formed. However, they were smaller and remained exclusively in the cell periphery. β4 integrin formed patches around these residual FAs but lacked the characteristic chevron shape. Quantitative comparison of FA and HD adhesion areas (Figure 5c) showed that both were reduced at early time points after seeding reaching control levels later, indicating less efficient adhesion.

We then investigated how, conversely, the distribution of FAs is affected by HD impairment. To this end, nHEKs were treated with blocking antibodies against α6 integrin (Figure 5b). Although β4 integrin-positive patches still remained in the cell periphery after this treatment, HD chevrons were completely absent until 75 minutes after seeding. By 165 minutes, HD chevrons started to form, but were smaller and less distinctive compared to those of untreated cells. Quantitative comparison of junctional adhesion areas (Figure 5d) showed that α6 integrin blocking antibodies significantly reduced FA and HD areas 75 and 165 minutes after seeding. Taken together, the observations suggest that a crosstalk between FAs and HDs is needed for the formation of ordered HD chevrons with intercalated FAs.

Migrating nHEKs secrete laminin-332 along their migration path and laminin-332–rich substrate enhances keratinocyte migration by accelerating FA/HD chevron formation

To explore the idea that keratinocytes secrete laminin-332 to form proper HDs, immunofluorescence microscopy was performed. Images of migrating nHEKs 36 hours after seeding showed that laminin-332, along with β4 integrin, is deposited at the cell front and is left behind marking the migration path (Figure 6a–6c).

To test whether prior laminin-332 deposition has an effect on migratory behavior, nHEKs were separately seeded on laminin-332-rich 804G cell-derived matrix (Spinardi et al., 1995) and fibronectin-coated matrix. Immunofluorescence images of FAs and HDs revealed that formation of mature chevrons and cell polarization were accelerated in nHEKs grown on laminin-332-rich matrix (Figure 6d, 6g). To study the effect on cell migration, single nHEK motility was monitored in time-lapse images. Tracking revealed drastically increased directionality and speed of migration on the laminin-332–rich matrix (Figure 6e, 6f, 6h, and 6i).

Hemidesmosomal chevron patterns are formed in the leader cells of collectively migrating keratinocytes

To examine whether chevron-like superstructures can be observed in cells during collective migration, nHEKs were grown within a removable barrier until confluent. Four hours after removing the barrier, collectively migrating cells were subjected to immunofluorescence analysis. The resulting images revealed that leader cells expressed typical intercalating FA-HD chevron patterns extending in the direction of migration, whereas follower cells did not (Figure 7). In accordance, confluent monolayers were also negative for chevron patterns (Supplementary Figure S3 online).

DISCUSSION

Our study uncovers a spatially and temporally coordinated, unique chevron-like organization of HDs with aligned FAs in migrating primary human keratinocytes that has not been reported so far, and differs from the less structured and more localized cat paw pattern described in other migrating epithelial cells (Colburn and Jones, 2018; Tsuruta et al., 2003; see also (Geuijen and Sonnenberg, 2002, Spinardi et al., 2004). We observed a very similar pattern in keratinocytes growing on micropatterned fibronectin-coated X-shapes, during cell spreading and, most importantly, in leader cells of collectively migrating sheets. All situations are characterized by highly localized stresses, as evidenced by the restricted distribution of actin stress-fiber associated force-bearing FAs (De Pascalis et al., 2018; van Hoorn et al., 2014). Less-localized FA distribution occurring, for example, in keratinocytes on D-shaped micropatterns did not result in chevron pattern formation.

A major feature of the FA-HD chevrons is their coordinated treadmilling with assembly occurring at the leading front of the cell and disassembly near the cell rear. It is unlikely that de novo synthesis and degradation of all polypeptide components or diffusion of components suffice to support the treadmilling. Instead, transport machinery is probably involved, which takes up components at the cell rear and delivers them at the cell front. An exciting finding in this context is the recent observation of Arf6-dependent trafficking of hemidesmosomal integrins in human keratinocytes (Osmani et al., 2018). Even more, the proposed stretch-induced α6β4 integrin delivery may explain how HDs are formed next to actin stress fiber-associated FAs in migrating keratinocytes. This mechanism would pave the way to couple environmental probing with persistent HD-supported cell migration.

Despite treadmilling, FAs and HDs remain in place the entire time between assembly and disassembly, although size changes occur, and intrinsic polypeptide turnover likely occurs throughout (Geuijen and Sonnenberg, 2002; Tsuruta et al., 2003). The overall structural persistence of the FA-decorated hemidesmosomal arrays suggests that they provide leverage for the associated cytoskeletal filaments to translocate the cell body over the substrate in the direction of migration. The tension forces needed for pulling the composite and highly flexible keratin network, together with nucleus and other cellular components, is provided by the actomyosin system (Lauffenburger and Horwitz, 1996; Le Clainche and Carlier, 2008; Sheetz et al., 1998).

Our observations differ from previous reports, which investigated the relationship between HDs and FAs in migrating rat 804G urothelial cells and immortalized human

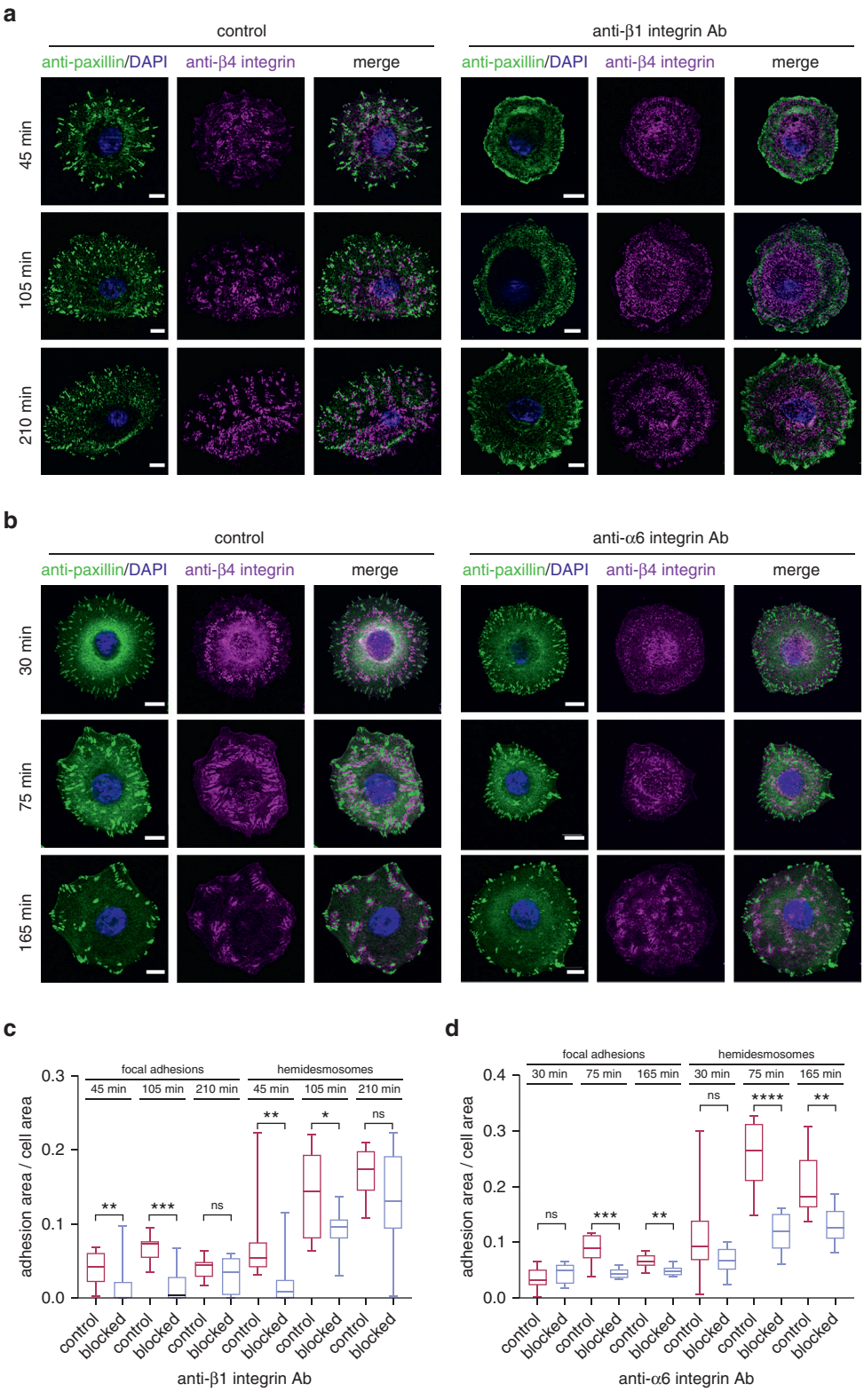

Figure 5. Hemidesmosomal chevrons and focal adhesions affect each other during substrate adhesion. Immunodetection of β4 integrin and paxillin in single normal human epithelial keratinocytes at different times after seeding. (**a**) Treatment with anti-β1 integrin–blocking antibodies induces peripheral localization of smaller focal adhesions and prevents hemidesmosomal chevron formation. (**b**) Treatment with anti-α6 integrin antibodies inhibits hemidesmosomal chevron formation and restricts focal adhesions to the cell periphery. Scale bars = 10 μm. (**c**–**d**) Box plots show average areas of focal adhesions and hemidesmosomes per cell at different time points in the presence or absence of blocking antibodies. Note that anti-β1 integrin and anti-α6 integrin significantly reduce both focal adhesion and hemidesmosome areas 45/105 minutes and 75/165 minutes after seeding, respectively. Mann-Whitney *t* test, n = 10, $*P < 0.05$, $**P < 0.01$, $***P < 0.001$.

keratinocytes (Ozawa et al., 2010; Tsuruta et al., 2003). We were not able to detect movement of either FAs or HDs with respect to the substrate. Most importantly, we did not observe sequential occupation of FA adhesion sites by hemidesmosomal proteins. Instead, FAs and HDs remained in place without spatial overlap or detectable exchange between both. Our observations therefore do not support the "substitution" model proposed by Tsuruta et al. (2011) (Ozawa et al., 2014; see also Spinardi et al., 2004), whereby FAs prepare a specialized membrane domain that is subsequently populated by hemidesmosomal proteins. Instead, we propose a "linkage" model, which posits that HD

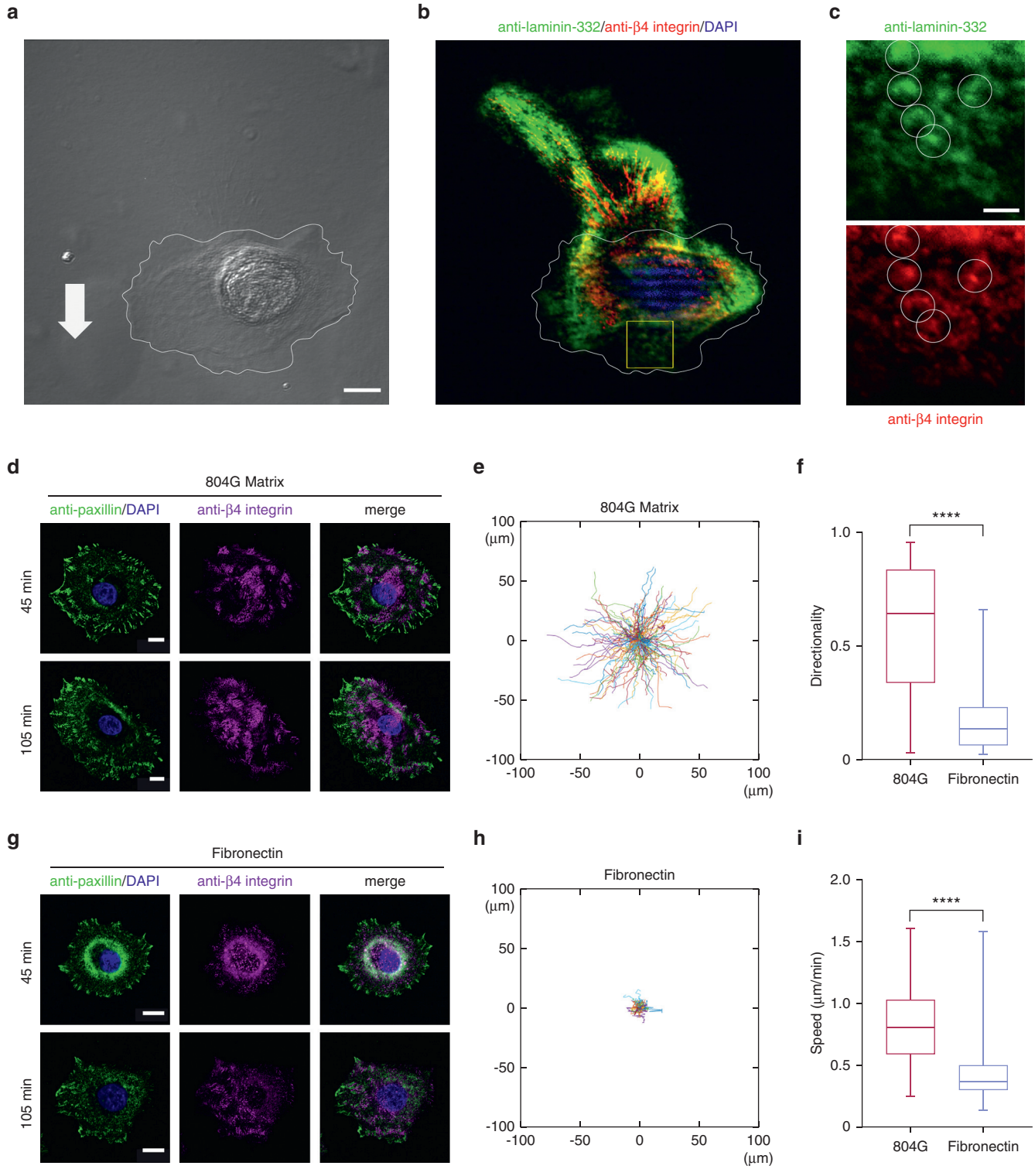

Figure 6. Laminin-332 is secreted by migrating keratinocytes and accelerates hemidesmosome formation and migration. The phase contrast (**a**) and fluorescence images (**b, c**) were recorded 36 hours after seeding on a fibronectin-coated glass coverslip. The arrow shows the direction of migration. Note that laminin-332 is deposited on the substrate at the leading edge co-localizing with β4 integrin and is left behind at the cell rear. (**d, g**) The immunofluorescence images of single normal human epithelial keratinocytes at different time points on either fibronectin-coated or laminin-332–rich 804G-derived matrix. Note the accelerated maturation of focal adhesion-hemidesmosome chevrons and polarization in normal human epithelial keratinocytes cultured on 804G matrix. (**e, h**) Track plots of normal human epithelial keratinocytes migrating on either 804G-derived matrix or fibronectin. Normal human epithelial keratinocytes were seeded at low density on either matrix and were allowed to attach for 200 minutes prior to motility tracking. Each line represents the track of a single cell over 20 time points (recording interval: 180 seconds). The starting point of each track was normalized to x = 0 and y = 0. (804G: n = 181, fibronectin: n = 70) (**f**) shows the deduced directionality of migration and (**i**) the speed of migration. Mann-Whitney *t* test, ****$P < 0.0001$.

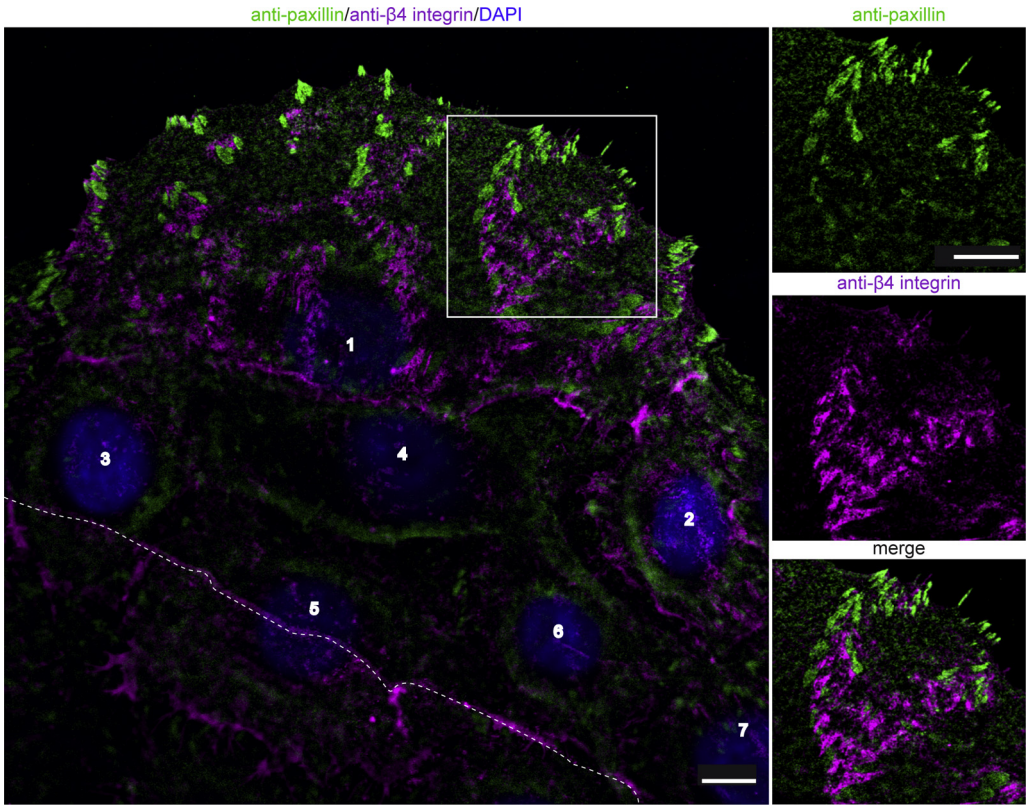

Figure 7. Hemidesmosomal chevrons are expressed at the leading front of collectively migrating cells. Fluorescence confocal microscopy of the front of collectively migrating normal human epithelial keratinocytes 4 hours after insert removal detecting paxillin-positive focal adhesions and β4 integrin-positive hemidesmosomes. Note that only leader cell 1 shows abundant focal adhesion-hemidesmosome chevron patterns, whereas the following cells 2−7 do not. Focal adhesion-hemidesmosome chevrons are extended in the direction of cell migration with focal adhesion formation slightly preceding hemidesmosome formation. The initial border of the insert is demarcated by accumulation of β4 integrin (dotted line). Scale bars = 10 μm.

formation occurs in close proximity of FAs through mechanisms involving spatial, mechanical or biochemical cues. FAs play a central role in both models, however, by facilitating intimate ECM attachment of a plasma membrane patch. The proponents of the substitution model further hypothesized that α6/β4 integrins interact with actin filaments prior to HD formation (Spinardi et al., 2004; Tsuruta et al., 2011). We did not find evidence for this mechanism in either migrating or spreading keratinocytes. Instead, the latter process provided strong evidence for immediate linkage of keratin intermediate filaments to nascent HDs without prior engagement of actin filaments. A major reason for the discrepancies between the previous studies (e.g., Geuijen and Sonnenberg, 2002; Spinardi et al., 2004; Tsuruta et al., 2003) and our current study may be that the previously used cell systems, which employed transformed or immortalized epithelial cells, do not support the formation of the conspicuous FA-studded hemidesmosomal chevron patterns that we detected in primary nHEKs. Fully mature FA-HD chevrons may be needed to form stable ECM connections, in the absence of which slippage occurs.

An important outcome of our experiments is that the relationship between FAs and HDs is not purely hierarchical but that it is also mutual. Thus, FAs are obviously a prerequisite for the formation of hemidesmosomal chevron arrays and, conversely, HDs are also needed for FA maturation and localization. The crosstalk between HDs and FAs likely involves different mechanisms.

Sterical facilitation. FAs may be needed to bring the adjacent plasma membrane in ideal apposition to the ECM to promote α6/β4 integrin clustering.

Mechanical linkage. Structural proteins, such as plectin, with its long rod domain (cf. Wiche and Winter, 2011), or actomyosin fibers may bridge the space between FAs and HDs by directly binding to components of both junctions.

Ligand competition. It is known that FA α3/β1 integrins and HD α6/β4 integrins compete for the ECM ligand laminin-332 (Baker et al., 1996; Mizushima et al., 1997). In addition, the cytoskeletal cross-linker plectin associates with FAs and HDs (Geerts et al., 1999; Litjens et al., 2006), as do the tetraspanin CD151 (Penas et al., 2000; Sterk et al., 2000, Winterwood et al., 2006) and actinin family members (Gonzalez et al., 2001; Hamill et al., 2013, 2015; Hiroyasu et al., 2016; Otey et al., 1990). The alternative associations may allow localization of the respective FA and HD components to juxtaposed plasma membrane regions, where the individual components will then be sorted locally according to binding strength to either junction and its respective components.

Signaling. Recent observations have provided evidence that mechanical signals are involved in HD formation (Osmani

et al., 2018). Such mechanical signals may be elicited by FA-attached actin stress fibers. Alternatively, the FA proteins kindlin and syndecan have been implicated in regulating hemidesmosome protein localization (Hopkinson et al., 2014; Larjava et al., 2008; Wang et al., 2010). The signaling crosstalk is apparently bidirectional, involving α6β4 integrin signaling through Rac1 (Colburn and Jones, 2018; Russell et al., 2003; Sehgal et al., 2006) and may even extend to biosynthetic regulation as α6β4 integrin–dependent activation of the Akt-mTOR pathway affects synthesis of α2 and α3 integrins (Kligys et al., 2007, 2012).

An interesting consideration in trying to understand the peculiar pattern of FA-HD arrangement is their differing affinity to fibronectin versus laminin-332. The FA integrins, notably α5/β1, bind preferentially to fibronectin, whereas the hemidesmosomal integrin dimer α6/β4 binds to laminin-332 (Hopkinson et al., 2014). Therefore, coating the glass slide with fibronectin provided a suitable matrix for FAs only. Our observation of laminin-332 deposition at the leading front of migrating nHEKs and co-distribution of β4 integrin (Figure 6) provides evidence that laminin-332 is secreted to support HD formation on fibronectin matrix. This is in agreement with the reported deposition of laminin-322 during wound healing (Goldfinger et al., 1999; Nguyen et al., 2000).

Furthermore, migrating cells leave laminin-332–rich streaks and membrane-containing macroaggregates behind, which serve as tracks for following cells (Figures 2a, 6b) (Geuijen and Sonnenberg, 2002; Rigort et al., 2004). Type I macroaggregates contain FA integrin β1 and type II macroaggregates contain hemidesmosomal integrin β4. The macroaggregates are generated by ripping off retraction fibers. The different types of macroaggregates are spatially segregated with FA-derived structures forming spherical and tubular structures in a "pearls on a string" arrangement, whereas HD-derived structures are spherical and fill the space in between. In this way, the ECM retains a mold of the FA-HD arrangement that can be used by follower cells (Rigort et al., 2004). A reflection of this feature may be the highly organized supracellular HD arrangement in native tissues (Owaribe et al., 1990, 1991).

What are the advantages of the ordered FA-HD chevron pattern? (i) HDs stabilize FA positioning and regulate FA density, which has been shown to modulate actin flow (Mohl et al., 2012), affecting speed and persistence of migration (Maiuri et al., 2015); (ii) the polarized nature of the chevrons reinforces migration persistence; and (iii) the coordination of FAs and HDs supports coordinated cytoskeletal remodeling and dynamics. The unique properties of the FA-HD chevron pattern become particularly important in coordinated collective cell migration requiring highly ordered force distribution and cytoskeletal–junction interactions in leader and follower cells (De Pascalis and Etienne-Manneville, 2017; De Pascalis et al., 2018; Vishwakarma et al., 2018).

MATERIALS AND METHODS

Cell culture

nHEKs from neonatal foreskin were purchased from Cell Systems (Kirkland, WA). Details on growth conditions, drug treatments, and antibody blocking experiments are provided in the Supplementary Material. Patient consent for the experiments was not required because all cells used for the experiments were acquired via accredited, commercially available source.

Immunofluorescence microscopy

Detailed protocols and a complete list of antibodies and dyes are provided in the Supplementary Material and Supplementary Tables S1, S2, S3.

Transfections and constructs

Cells were transiently transfected 1 day after seeding with transit-keratinocyte transfection reagent (Mirus Bio, Madison, WI). A total amount of 2.5 μg DNA was mixed with 3.75 μl reagent and 250 μl medium for each 35-mm–diameter dish.

The paxillin-pDsRed2-N1 construct encoding paxillin-DsRed2 was kindly provided by Rick Horwitz (Webb et al., 2004). A construct encoding the GFP-β4 integrin fusion protein GFP-hb4 was kindly provided by Jonathan Jones (Tsuruta et al., 2003).

Micropatterning

Deep-UV micropatterning was performed according to the protocol described in Azioune et al. (2010) and as detailed in Supplementary Material.

Imaging

Structured Illumination Microscopy for Optical Sectioning (OS-SIM) was performed with an ApoTome.2.microscope (Zeiss, Oberkochen, Germany) equipped with an oil immersion objective ×63 (N.A. 1.4, DIC, Plan apochromat). Live-cell imaging and imaging of immunostained samples were done using an LSM 710 DUO confocal microscope (Zeiss) equipped with a DefiniteFocus device (Zeiss) and an oil immersion objective ×63 (N.A. 1.4, DIC M27). Live-cell imaging was performed in a humidified chamber with 5% CO_2 at 37°C.

Image Analysis

Fiji software (Schindelin et al., 2012) was used to track cell motility and to quantify adhesion areas. Detailed protocols are provided in the Supplementary Material.

DATA AVAILABILITY

The data that support the findings of this study are available from the corresponding author, RL, upon reasonable request.

ORCIDs

Anne Pora: https://orcid.org/0000-0002-0276-6267
Sungjun Yoon: https://orcid.org/0000-0001-7363-3261
Reinhard Windoffer: https://orcid.org/0000-0003-1403-5880
Rudolf Eberhard Leube: https://orcid.org/0000-0002-5519-7379

CONFLICT OF INTEREST

The authors state no conflict of interest.

ACKNOWLEDGMENTS

We thank Jonathan Jones (Washington State University, Pullman), Rick Horwitz (Allen Institute for Cell Science, Seattle), Monique Aumailley (University of Cologne), Staffan Johansson (University of Uppsala), and Harald Herrmann (German Cancer Research Center) for valuable plasmids and antibodies. This project has received funding from the European Union's Horizon 2020 research and innovation program under the Marie Skłodowska-Curie grant agreement No 642866.

AUTHOR CONTRIBUTIONS

Conceptualization: AP, SY, RW, RL; Data Curation: AP, SY, RW; Formal Analysis: AP, SY, RW; Funding Acquisition: RW, RL; Investigation: AP, SY; Project Administration: RW, RL; Software: RW; Supervision: RW, RL; Visualization: AP, SY, RW, RL; Writing — Original Draft: AP, SY, RL; Writing — Review & Editing: AP, SY, RW, RL

SUPPLEMENTARY MATERIAL

Supplementary material is linked to the online version of the paper at www.jidonline.org, and at https://doi.org/10.1016/j.jid.2019.03.1139.

REFERENCES

Azioune A, Carpi N, Tseng Q, Thery M, Piel M. Protein micropatterns: a direct printing protocol using deep UVs. Methods Cell Biol 2010;97:133–46.

Baker SE, Hopkinson SB, Fitchmun M, Andreason GL, Frasier F, Plopper G, et al. Laminin-5 and hemidesmosomes: role of the alpha 3 chain subunit in hemidesmosome stability and assembly. J Cell Sci 1996;109(Pt 10): 2509–20.

Carter WG, Kaur P, Gil SG, Gahr PJ, Wayner EA. Distinct functions for integrins alpha 3 beta 1 in focal adhesions and alpha 6 beta 4/bullous pemphigoid antigen in a new stable anchoring contact (SAC) of keratinocytes: relation to hemidesmosomes. J Cell Biol 1990;111(6 Pt 2):3141–54.

Chaudhari PR, Vaidya MM. Versatile hemidesmosomal linker proteins: structure and function. Histol Histopathol 2015;30:425–34.

Colburn ZT, Jones JCR. Complexes of alpha6beta4 integrin and vimentin act as signaling hubs to regulate epithelial cell migration. J Cell Sci 2018;131(14).

De Pascalis C, Etienne-Manneville S. Single and collective cell migration: the mechanics of adhesions. Mol Biol Cell 2017;28:1833–46.

De Pascalis C, Perez-Gonzalez C, Seetharaman S, Boeda B, Vianay B, Burute M, et al. Intermediate filaments control collective migration by restricting traction forces and sustaining cell-cell contacts. J Cell Biol 2018;217:3031–44.

Geerts D, Fontao L, Nievers MG, Schaapveld RQ, Purkis PE, Wheeler GN, et al. Binding of integrin alpha6beta4 to plectin prevents plectin association with F-actin but does not interfere with intermediate filament binding. J Cell Biol 1999;147:417–34.

Geiger B, Yamada KM. Molecular architecture and function of matrix adhesions. Cold Spring Harb Perspect Biol 2011;3(5).

Geuijen CA, Sonnenberg A. Dynamics of the alpha6beta4 integrin in keratinocytes. Mol Biol Cell 2002;13:3845–58.

Goldfinger LE, Hopkinson SB, deHart GW, Collawn S, Couchman JR, Jones JC. The alpha3 laminin subunit, alpha6beta4 and alpha3beta1 integrin coordinately regulate wound healing in cultured epithelial cells and in the skin. J Cell Sci 1999;112(Pt 16):2615–29.

Gonzalez AM, Otey C, Edlund M, Jones JC. Interactions of a hemidesmosome component and actinin family members. J Cell Sci 2001;114(Pt 23): 4197–206.

Hamill KJ, Hiroyasu S, Colburn ZT, Ventrella RV, Hopkinson SB, Skalli O, et al. Alpha actinin-1 regulates cell-matrix adhesion organization in keratinocytes: consequences for skin cell motility. J Invest Dermatol 2015;135: 1043–52.

Hamill KJ, Hopkinson SB, Skalli O, Jones JC. Actinin-4 in keratinocytes regulates motility via an effect on lamellipodia stability and matrix adhesions. FASEB J 2013;27:546–56.

Hiroyasu S, Colburn ZT, Jones JC. A hemidesmosomal protein regulates actin dynamics and traction forces in motile keratinocytes. FASEB J 2016;30: 2298–310.

Hopkinson SB, Hamill KJ, Wu Y, Eisenberg JL, Hiroyasu S, Jones JC. Focal contact and hemidesmosomal proteins in keratinocyte migration and wound repair. Adv Wound Care (New Rochelle) 2014;3:247–63.

Kligys K, Claiborne JN, DeBiase PJ, Hopkinson SB, Wu Y, Mizuno K, et al. The slingshot family of phosphatases mediates Rac1 regulation of cofilin phosphorylation, laminin-332 organization, and motility behavior of keratinocytes. J Biol Chem 2007;282:32520–8.

Kligys KR, Wu Y, Hopkinson SB, Kaur S, Platanias LC, Jones JCR. alpha6beta4 integrin, a master regulator of expression of integrins in human keratinocytes. J Biol Chem 2012;287:17975–84.

Larjava H, Plow EF, Wu C. Kindlins: essential regulators of integrin signalling and cell-matrix adhesion. EMBO Rep 2008;9:1203–8.

Lauffenburger DA, Horwitz AF. Cell migration: a physically integrated molecular process. Cell 1996;84:359–69.

Le Clainche C, Carlier M-F. Regulation of actin assembly associated with protrusion and adhesion in cell migration. Physiol Rev 2008;88:489–513.

Litjens SH, de Pereda JM, Sonnenberg A. Current insights into the formation and breakdown of hemidesmosomes. Trends Cell Biol 2006;16:376–83.

Maiuri P, Rupprecht JF, Wieser S, Ruprecht V, Benichou O, Carpi N, et al. Actin flows mediate a universal coupling between cell speed and cell persistence. Cell 2015;161:374–86.

Mizushima H, Takamura H, Miyagi Y, Kikkawa Y, Yamanaka N, Yasumitsu H, et al. Identification of integrin-dependent and -independent cell adhesion domains in COOH-terminal globular region of laminin-5 alpha 3 chain. Cell Growth Differ 1997;8:979–87.

Mohl C, Kirchgessner N, Schafer C, Hoffmann B, Merkel R. Quantitative mapping of averaged focal adhesion dynamics in migrating cells by shape normalization. J Cell Sci 2012;125(Pt 1):155–65.

Nahidiazar L, Kreft M, van den Broek B, Secades P, Manders EMM, Sonnenberg A, et al. The molecular architecture of hemidesmosomes, as revealed with super-resolution microscopy. J Cell Sci 2015;128: 3714–9.

Nguyen BP, Gil SG, Carter WG. Deposition of laminin 5 by keratinocytes regulates integrin adhesion and signaling. J Biol Chem 2000;275: 31896–907.

Osmani N, Pontabry J, Comelles J, Fekonja N, Goetz JG, Riveline D, et al. An Arf6- and caveolae-dependent pathway links hemidesmosome remodeling and mechanoresponse. Mol Biol Cell 2018;29:435–51.

Otey CA, Pavalko FM, Burridge K. An interaction between alpha-actinin and the beta 1 integrin subunit in vitro. J Cell Biol 1990;111:721–9.

Owaribe K, Kartenbeck J, Stumpp S, Magin TM, Krieg T, Diaz LA, et al. The hemidesmosomal plaque. I. Characterization of a major constituent protein as a differentiation marker for certain forms of epithelia. Differentiation 1990;45:207–20.

Owaribe K, Nishizawa Y, Franke WW. Isolation and characterization of hemidesmosomes from bovine corneal epithelial cells. Exp Cell Res 1991;192:622–30.

Ozawa T, Hiroyasu S, Tsuruta D. The role of hemidesmosomes and focal contacts in the skin visualized by dual-color live cell imaging. Med Mol Morphol 2014;47:185–8.

Ozawa T, Tsuruta D, Jones JC, Ishii M, Ikeda K, Harada T, et al. Dynamic relationship of focal contacts and hemidesmosome protein complexes in live cells. J Invest Dermatol 2010;130:1624–35.

Penas PF, Garcia-Diez A, Sanchez-Madrid F, Yanez-Mo M. Tetraspanins are localized at motility-related structures and involved in normal human keratinocyte wound healing migration. J Invest Dermatol 2000;114:1126–35.

Rabinovitz I, Toker A, Mercurio AM. Protein kinase C-dependent mobilization of the alpha6beta4 integrin from hemidesmosomes and its association with actin-rich cell protrusions drive the chemotactic migration of carcinoma cells. J Cell Biol 1999;146:1147–60.

Rigort A, Grunewald J, Herzog V, Kirfel G. Release of integrin macroaggregates as a mechanism of rear detachment during keratinocyte migration. Eur J Cell Biol 2004;83:725–33.

Russell AJ, Fincher EF, Millman L, Smith R, Vela V, Waterman EA, et al. Alpha 6 beta 4 integrin regulates keratinocyte chemotaxis through differential GTPase activation and antagonism of alpha 3 beta 1 integrin. J Cell Sci 2003;116(Pt 17):3543–56.

Schindelin J, Arganda-Carreras I, Frise E, Kaynig V, Longair M, Pietzsch T, et al. Fiji: an open-source platform for biological-image analysis. Nat Methods 2012;9:676–82.

Sehgal BU, DeBiase PJ, Matzno S, Chew T-L, Claiborne JN, Hopkinson SB, et al. Integrin beta4 regulates migratory behavior of keratinocytes by determining laminin-332 organization. J Biol Chem 2006;281:35487–98.

Sheetz MP, Felsenfeld DP, Galbraith CG. Cell migration: regulation of force on extracellular-matrix-integrin complexes. Trends Cell Biol 1998;8:51–4.

Spinardi L, Einheber S, Cullen T, Milner TA, Giancotti FG. A recombinant tail-less integrin beta 4 subunit disrupts hemidesmosomes, but does not suppress alpha 6 beta 4-mediated cell adhesion to laminins. J Cell Biol 1995;129:473–87.

Spinardi L, Rietdorf J, Nitsch L, Bono M, Tacchetti C, Way M, et al. A dynamic podosome-like structure of epithelial cells. Exp Cell Res 2004;295:360–74.

Sterk LM, Geuijen CA, Oomen LC, Calafat J, Janssen H, Sonnenberg A. The tetraspan molecule CD151, a novel constituent of hemidesmosomes, associates with the integrin alpha6beta4 and may regulate the spatial organization of hemidesmosomes. J Cell Biol 2000;149:969–82.

Tsuruta D, Hashimoto T, Hamill KJ, Jones JC. Hemidesmosomes and focal contact proteins: functions and cross-talk in keratinocytes, bullous diseases and wound healing. J Dermatol Sci 2011;62:1–7.

Tsuruta D, Hopkinson SB, Jones JC. Hemidesmosome protein dynamics in live epithelial cells. Cell Motil Cytoskeleton 2003;54:122–34.

van Hoorn H, Harkes R, Spiesz EM, Storm C, van Noort D, Ladoux B, et al. The nanoscale architecture of force-bearing focal adhesions. Nano Lett 2014;14:4257–62.

Vishwakarma M, Di Russo J, Probst D, Schwarz US, Das T, Spatz JP. Mechanical interactions among followers determine the emergence of leaders in migrating epithelial cell collectives. Nat Commun 2018;9:3469.

Walko G, Castanon MJ, Wiche G. Molecular architecture and function of the hemidesmosome. Cell Tissue Res 2015;360:529–44.

Wang H, Leavitt L, Ramaswamy R, Rapraeger AC. Interaction of syndecan and alpha6beta4 integrin cytoplasmic domains: regulation of ErbB2-mediated integrin activation. J Biol Chem 2010;285:13569–79.

Webb DJ, Donais K, Whitmore LA, Thomas SM, Turner CE, Parsons JT, et al. FAK-Src signalling through paxillin, ERK and MLCK regulates adhesion disassembly. Nat Cell Biol 2004;6:154–61.

Wiche G, Osmanagic-Myers S, Castanon MJ. Networking and anchoring through plectin: a key to IF functionality and mechanotransduction. Curr Opin Cell Biol 2015;32:21–9.

Wiche G, Winter L. Plectin isofroms as organizers of intermediate filament cytoarchitecture. Bioarchitecture 2011;1:14–20.

Windoffer R, Beil M, Magin TM, Leube RE. Cytoskeleton in motion: the dynamics of keratin intermediate filaments in epithelia. J Cell Biol 2011;194:669–78.

Winterwood NE, Varzavand A, Meland MN, Ashman LK, Stipp CS. A critical role for tetraspanin CD151 in alpha3beta1 and alpha6beta4 integrin-dependent tumor cell functions on laminin-5. Mol Biol Cell 2006;17:2707–21.

Zaidel-Bar R, Geiger B. The switchable integrin adhesome. J Cell Sci 2010;123(Pt 9):1385–8.

Zaidel-Bar R, Itzkovitz S, Ma'ayan A, Iyengar R, Geiger B. Functional atlas of the integrin adhesome. Nat Cell Biol 2007;9:858–67.

SUPPLEMENTARY MATERIAL AND METHODS

Cell culture

nHEKs (Cell Systems) were grown in Dermalife K Medium Complete (Cell Systems) without TGFα to avoid differentiation and in the presence of penicillin-streptomycin (100 μg/ml). nHEKs were passaged using Trypkit (Cell Systems) for trypsinization. They could be frozen at any passage in Cryo-SFM freezing medium (Promocell, Heidelberg, Germany). Cells were routinely used for experiments at passage P3 corresponding to approximatively 10 population doublings. nHEKs were seeded at a density of 5,000 cells per cm^2 either on 24 mm-diameter high-precision glass coverslips (#1.5 from Marienfeld) that had been coated with human fibronectin (VWR) by a 30 minutes incubation in 1.5 ml of a solution containing 17 mg/l fibronectin at 37°C for high resolution confocal microscopy, on 12-mm−diameter coverslips (#1.5 from ThermoScientific, Waltham, MA) for structured illumination microscopy, or on 35 mm-diameter glass bottom dishes (MatTek, Ashland, MA) for live-cell imaging.

Collective cell migration assay

Thirty-five-millimeter μ-Dishes (Ibidi, Martinsreid, Germany) were first coated with human fibronectin using the method described. The culture-insert 2 well (Ibidi) was then attached to the dish and 70 μl of culture medium containing 20,000 cells were added immediately afterwards to each well of the insert. Cells were then grown for 24 hours and the insert was removed to initiate collective cell migration. Cell culture was continued for another 4 hours until paraformaldehyde-acetone fixation.

Drug treatments and antibody blocking experiments

The following antibodies were used in blocking experiments: anti-β1 integrin (polyclonal, 1:200, rabbit, kindly provided by Staffan Johansson (Maschler et al., 2005) and anti-α6 integrin CD49f clone GoH3 (1:100, IgG2a, rat; Beckman Coulter IM0769). For antibody blocking experiments, 10,000 cells were suspended in 100 μl medium with the antibodies and subsequently seeded on a fibronectin-coated glass coverslip.

Immunofluorescence microscopy

Fixation was performed without any prior washing steps in order to avoid cell contraction. Two different fixation methods were used: (i) For methanol-acetone fixation, cells were fixed for 2 minutes in methanol at −20°C and immediately permeabilized in acetone at −20°C for 20 seconds. (ii) For paraformaldehyde-acetone fixation, cells were first fixed for 10 minutes at room temperature in 4% (w/v) paraformaldehyde (Merck, Kennilworth, NJ) in phosphate buffered saline and were then permeabilized in acetone at −20°C for 30 seconds.

For staining, fixed cells were saturated for 20 minutes at room temperature in a solution containing 5% (w/v) bovine serum albumin (Serva, Heidelberg, Germany) in phosphate buffered saline. Incubation with primary antibodies in a solution of 1% bovine serum albumin in phosphate buffered saline was performed for 90 minutes at room temperature and followed by three washing steps in phosphate buffered saline. Incubation with the secondary antibodies suspended in phosphate buffered saline with 1% bovine serum albumin was performed for 35 minutes at room temperature and followed by three washing steps. When phalloidin was used, it was mixed with the primary antibodies. When DAPI (Supplementary Table S3) was used, it was mixed with the secondary antibodies. Mounting reagent was Mowiol (Carl Roth, Karlsruhe, Germany).

Quantification of adhesion areas

Structured Illumination Microscopy for Optical Sectioning (OS-SIM) was performed with an ApoTome.2.microscope (Zeiss) equipped with an oil immersion objective ×63 (N.A. 1.4, DIC, Plan apochromat). Images were recorded from 10 single cells for each experimental condition.

For segmentation of cells, Fiji plugin WEKA (Arganda-Carreras et al., 2017) was used. Three separate classifiers were trained using representative images from the recordings to discretize FAs, HDs, and cell body from background. These classifiers were used for segmentation of all images. In some cases "Huang dark" thresholding was used for cell body detection. Next, the Fiji routine "Analyze particles" was applied to remove structures of unwanted size, that is, cell groups, clutter, and structures with a circularity <0.1, and to determine the area data of the defined target particles.

The resulting data were further analyzed with GraphPad Prism 7 software (GraphPad, La Jolla, CA) to quantitatively compare adhesion areas per cell of cells treated with blocking antibodies and untreated control cells.

Micropatterning

Deep-UV micropatterning according to the protocol of (Azioune et al., 2010) was performed as follows. High precision coverslips (24-mm diameter) were spin-coated with TI PRIME (MicroChemicals, Ulm, Germany), then with polystyrene (Sigma-Aldrich, St Louis, MO). Afterwards, they were exposed to deep UV. They were incubated in poly(L-lysine)−grafted poly(ethylene glycol) (Surface Solutions, Maplewood, NJ), and then exposed to deep UV using a mask manufactured by Compugraphics (Watertown, CT). The coverslips were then incubated in 100 mM $NaHCO_3$ supplemented with human fibronectin (5 μg/μl). Finally, nHEKs were seeded at a density of 6,600 cells per cm^2.

Laminin-332−rich 804G matrix preparation

Laminin-332−rich matrix was prepared using 804G cells (Langhofer et al., 1993). The cells were cultured for 3−4 days until confluent on surfaces to be coated, and were then detached by incubating in cold (4°C) 20 mM NH_4OH for 10 minutes. The solution was then discarded, followed by three washing steps with distilled water to remove all remaining debris. Finally, surfaces were washed with phosphate buffered saline without Ca^{2+}/Mg^{2+} and stored at −28°C for up to 2 months before use.

Tracking of migrating cells

nHEKs were seeded on fibronectin- or 804G-derived matrix-coated glass-bottom dishes at low density. Interference contrast images were recorded using the transmission detector of an LSM 710 confocal microscope. Images were recorded from nine positions every 180 seconds using oil

immersion objective ×63 (N.A. 1.4, DIC M27). A total of 75 time points was used for each analysis.

For segmentation of cells, the Fiji plugin WEKA (Arganda-Carreras et al., 2017) was used as described for quantification of adhesion areas to discretize between cells and background. Tracks of cells were detected using the Fiji plugin TrackMate. Cells were identified using the LoG detector and the simple LAP tracker was used for tracking. The resulting data were further analyzed with custom-written Matlab routines and with GraphPad Prism, version 7. Only the first 20 time points of each track were considered.

SUPPLEMENTARY REFERENCES

Arganda-Carreras I, Kaynig V, Rueden C, Eliceiri K, Schindelin J, Cardona A, et al. Trainable Weka Segmentation: a machine learning tool for microscopy pixel classification. Bioinformatics 2017;33:2424–6.

Azioune A, Carpi N, Tseng Q, Thery M, Piel M. Protein micropatterns: a direct printing protocol using deep UVs. Methods Cell Biol 2010;97:133–46.

Langhofer M, Hopkinson SB, Jones JC. The matrix secreted by 804G cells contains laminin-related components that participate in hemidesmosome assembly in vitro. J Cell Sci 1993;105:753–64.

Maschler M, Gerhard W, Spring H, Bredow D, Sordat I, Beug H, et al. Tumor cell invasiveness correlates with changes in intergrin expression and localization. Oncogene 2005;24:2032–41.

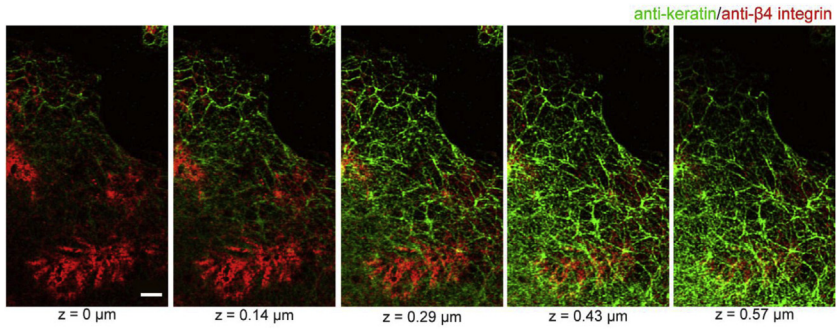

Supplementary Figure S1. Keratin filaments associate with hemidesmosomal chevrons in migrating keratinocytes. The pictures depict the immunofluorescence in successive 0.1435-μm–thick focal planes of the peripheral part of a fixed migrating normal human epithelial keratinocyte stained for β4 integrin and keratin (for corresponding maximum intensity projection images see Figure 1e). Scale bar = 2.5 μm.

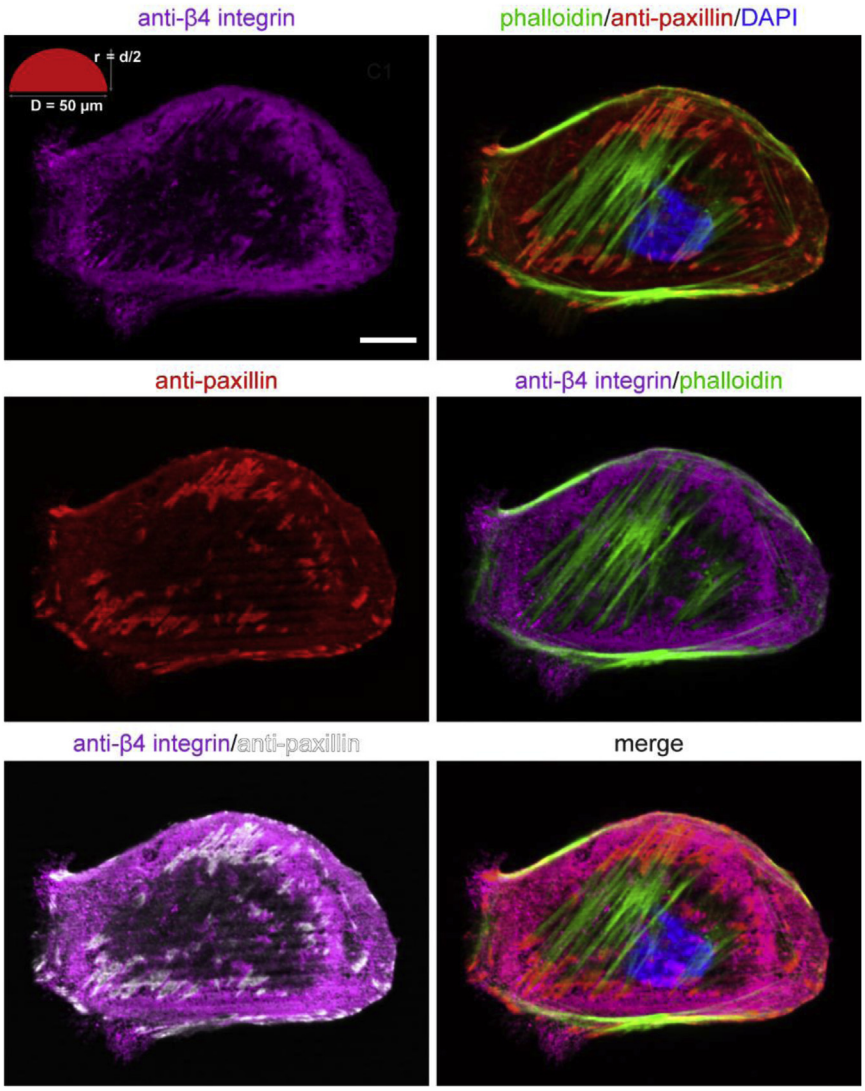

Supplementary Figure S2. Hemidesmosomes and focal adhesions are non-overlapping and intercalated on micropatterned D-shapes. Quadruple epifluorescence of a single paraformaldehyde-acetone fixed normal human epithelial keratinocytes that had grown for 1 day on a fibronectin-coated half-circle micropattern (dimensions in upper left micrograph). Actin was detected with phalloidin-Alexa 488 nm, nuclear DNA was labeled with DAPI, and staining for β4 integrin and paxillin was done with antibodies. Note that the β4 integrin signal is sandwiched between focal adhesions (false white in lower left image) at the outermost cell periphery next to the cortical actin and actin stress fiber-associated focal adhesions located in the more central part of the cell.
Scale bar = 10 µm.

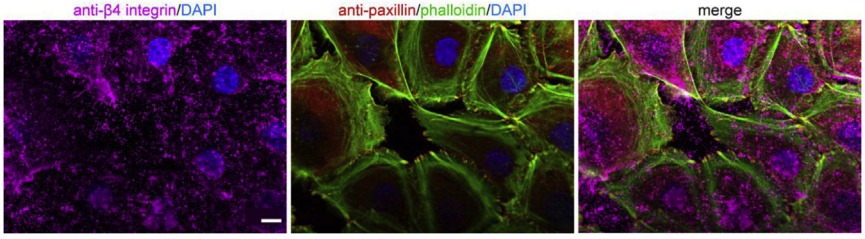

Supplementary Figure S3. Spatial linkage between hemidesmosomes and focal adhesions is not apparent in confluent keratinocytes. Shown are immunofluorescence images (epifluorescence) of confluent normal human epithelial keratinocytes seeded on fibronectin-coated glass coverslips and fixed with paraformaldehyde-acetone 7 days after seeding. Staining for β4 integrin and paxillin was performed with antibodies. Note that hemidesmosomal chevron patterns with intercalated focal adhesions cannot be detected.
Scale bar = 10 µm.

Supplementary Table S1. Primary antibody

Protein Target	Antibody Name	Manufacturer/Catalogue Number/ Name of Individual Providing Antibody	Species Raised	Dilution Used
Integrin β4	CD104 clone 439-9B	BD Pharmingen, 55719	Rat	1:300
Integrin β1	Anti-integrin β1	Staffan Johansson	Rabbit	1:200
Integrin α6	CD49f clone GoH3	Beckman Coulter, IM0769	Rat	1:100
Pan keratin	PAN-CK	ThermoFisher MA5-13203	Mouse	1:180
Paxillin	Clone 349	BD Biosciences, 610051	Mouse	1:100
Plectin	Anti-plectin	Harald Herrmann	Mouse	1:100
BPAG1	BP230 clone 279	CosmoBio NU-01-BP1	Mouse	1:100
Laminin-332	Anti-laminin-332	Monique Aumailley	Rabbit	1:5,000

Supplementary Table S2. Secondary antibody

Antibody Name	Manufacturer/ Catalogue Number	Dilution Used
Alexa-555 goat anti-rat IgG (H+L)	Invitrogen, A-21434	1:200
DyLight TM 405 donkey anti-rat IgG (H+L)	Jackson-Dianova, 712-476-153	1:100
Alexa-633 goat anti-mouse IgG (H+L)	Invitrogen, A-21053	1:500
Alexa-488 goat anti-mouse IgG (H+L)	Invitrogen, A-11029	1:1 000
Alexa-488 goat anti-guinea pig IgG (H+L)	Invitrogen, A-11073	1:1 000
Alexa-488 goat anti-rabbit IgG (H+L)	Invitrogen, A-11070	1:1 000

Supplementary Table S3. Additional dyes

Dye Name	Manufacturer/ Catalogue Number	Dilution Used
Alexa-Fluor-488 phalloidin	Invitrogen, A12379	1:100
DAPI	Roche, 10236276001	2 ng/μL